A novel technique for Residence Time Distribution (RTD) measurements in solids unit operations

Atena Dehghani Kiadehi, Mikel Leturia, Franco Otaola, Aïssa Ould-Dris, Khashayar Saleh

A novel technique for Residence Time Distribution (RTD) measurements in solids unit operations

Atena Dehghani Kiadehi, Mikel Leturia*, Franco Otaola, Aissa Ould-Dris, Khashayar Saleh

Sorbonne Universités, Université de Technologie de Compiègne, EA TIMR 4297 UTC, Rue du Dr Schweitzer, 60200 Compiègne, France

*Corresponding author: mikel.leturia@utc.fr

Abstract

This work presents a novel technique with fast response for Residence Time Distribution (RTD) measurements in gas-solid unit operations (*e.g.*, fluidized bed reactors). This technique is based on an optical method which eliminates the requirement of knowing the velocity and concentration profiles at the exit section of the system. Experiments were carried out with SiC particles and a phosphorescent pigment used as a tracer. A concentration measurement system was developed to measure the tracer concentration in SiC/pigment mixtures. The corresponding pigment concentrations were evaluated at the bottom of this system using a photomultiplier. The pigment concentration was derived from the integral of the signal intensity received by the photomultiplier. Then, a calibration curve was established which provided the empirical relationship between the integral and pigment concentration. In order to validate this RTD measurement technique, a series of experiments was performed in a bubbling fluidized bed and the effect of the bed height was studied. It was shown that the experimental RTD curves were in good agreement with the theoretical RTD of bubbling fluidized beds. This solids RTD measurement technique can be used to provide a better understanding of the hydrodynamics of complex solids unit operations.

Keywords: *Residence Time Distribution; Bubbling Fluidized Bed; Phosphorescent Pigment; Optical Method*

1. Introduction

In the study and design of solids unit operations, characterization of the overall flow behavior and mixing by means of solid Residence Time Distribution (RTD) are major issues. The solids flow patterns in these units are very complex. The solids in a continuous operation leave the system after a period of time approximating its mean residence time. Consequently, in solids unit operations there can be a broad range of residence times, which can be a serious concern if, as in many commercial applications, good control of solids mixing and uniform treatment of solids is desired [1].

The RTD does not carry complete information about the flow and structure of a particular unit operation. Nevertheless, it is possible to affirm that the RTD is a characteristic of the overall flow behavior and mixing which occur in the solids unit operations and are vital for solids unit operation design and scale-up, plant operation and optimization [2].

Fluidized bed reactors are present in many applications and gas-solid processes. These reactors are widely spread in numerous industries such as biomass gasification, reforming and chemical looping combustion [3-5]. The process efficiency in such processes depends on the contact efficiency and contact time between gas and solid particles. Therefore, knowledge of solid mixing and RTD is essential in order to describe, design and model fluidized bed reactors.

The residence time distribution function, *E(t)*, and the cumulative distribution function, *F(t)* for an instantaneous tracer injection or Dirac pulse input are defined as [6]:

$$E(t) = \frac{C(t)}{\int_0^\infty C(t)dt} \qquad \text{Eq. (1)}$$

$$F(t) = \int_0^t E(t)dt \qquad \text{Eq. (2)}$$

where *C(t)* is the tracer concentration at time *t*.

The mean residence time (t_m), which corresponds to the average of the residence times, is given by the first moment of the distribution *E(t)*:

$$t_m = \int_0^\infty t\, E(t)\, dt \qquad \text{Eq. (3)}$$

The essential requirement of fluidized bed reactors is to have a uniform contact between gas and solid phases. It is commonly accepted that it behaves as a continuously stirred tank reactor (CSTR) for solid phase. For good mixing, the RTD of the solid phase should be similar to that of an ideal CSTR. The residence time distribution function of an ideal CSTR (continuous stirred tank reactor) is defined as [6]:

$$E(t) = \frac{1}{\tau} \cdot e^{-t/\tau} \qquad \text{Eq. (4)}$$

where, τ is the space time (s) obtained by dividing solid volume in the reactor (V) by the solids volumetric flow rate entering the reactor (Q). In practice, it is calculated as the mass of solids in the fluidized bed (M_s) divided by the solids mass flow rate ($\dot{m}$):

$$\tau = \frac{V}{Q} = \frac{M_s}{\dot{m}} \qquad \text{Eq. (5)}$$

Several tracer methods have been used for solids RTD measurement. These methods are summarized in Table 1. Generally, the difficulties encountered when solid RTD measurements are required are caused by the size and density distributions of particles. On the other hand, the solids concentration is not uniform in the outlet section and the gas and solid velocities may be different.

From the review of the reported experimental methods, several research groups [1, 2, 22, 25-29] preferred to employ phosphorescent tracer particles, thanks to its simplicity and high accuracy. In these works, the properties of phosphorescent tracer particles were similar to the average properties of the fluidized bed particles.

Wei et al [27] made RTD measurements in a co-current down-flow circulating fluidized bed using phosphorescent tracer particles. Tracer mixtures were prepared with alumina, containing a small amount of fine phosphorescent particles as the tracer. Chen et al. [29] also chose a method of light

transmission using fluorescence to study solids RTD in extruders. A He-Ne laser was used as a light source. From the experimental results, they concluded that the light transmission method gave good RTD curves with an uncertainty of 6% on the average residence time.

The optical method has been perfected by Harris et al. [1, 2, 25]. In these phosphorescent tracer experiments, phosphorescent particles were used as both bulk and tracer particles. In fact, just a small amount of phosphorescent particles were illuminated and activated as a tracer. The detection was then carried out without disturbance of the hydrodynamic behavior by means of a light detector. In these works, the phosphorescent tracer particle consumption was quite high due to the large amount of the fluidized particles (bulk particles). In order to avoid this problem, a pneumatic injection of phosphor tracer technique (PIPTT) was proposed by Du et al. [22]. A similar technique was undertaken by Huang et al. [26]. An amount of phosphorescent tracer particles with properties similar to the bulk particles were injected into the fluidized bed, so wasteful amounts of phosphorescent particles were reduced significantly.

Since the intensity of the light emitted by the activated tracer decays with time, there is an upper residence time limit for phosphorescent tracer techniques (for example *3min* for the tracer particle used by Harris et al. [1]). Therefore, the solids RTD measurements using this technique have been extensively studied in short solids residence time units (*e.g.,* riser and downer of fluidized beds).

In summary, developing an accurate technique able to detect very low tracer concentrations is a non-trivial matter but is required to accurately characterize the solids RTD in unit operations with long residence times. Indeed, by detecting very low concentrations, the tracer consumption would be reduced, and the hydrodynamic pattern of the unit operation would be modified as little as possible. It must be noted that such a technique also eliminates the requirement of knowing the velocity and concentration profiles at the exit section of the system and is therefore more accurate than conventional methods.

The main purpose of this study was to develop a technique able to accurately detect very low tracer concentrations, allowing experimental RTD studies with extended residence times to be carried out without disturbing the hydrodynamics of the studied system. This technique was applied to a bubbling fluidized bed reactor and the results were validated by comparison with a theoretical model.

2. Materials and Methods

2.1. Materials

Experiments were carried out with SiC (Silicon carbide) used as bulk particles and a phosphorescent pigment (Lumilux® Green SN-F50 WS) used as a tracer. The tracer particles were chosen to have fluidization properties similar to the SiC particles. The particle size distributions and densities were studied using a laser granulometer Mastersizer 2000 (Malvern Instruments) and a helium pycnometer Accupyc 1330 (Micrometrics), respectively. The properties of the SiC and pigment particles are summarized in Table 2. The median diameter D50 is defined as the diameter where half of the population lies below this value. Similarly, 90 percent of the distribution lies below the D90, and 10 percent of the population lies below the D10.

This pigment absorbs photons in the UV range and emits photons in the visible range. The peak of the excitation spectrum is in the UV zone (*360-380nm*) of the spectrum, whereas the emission peak is in the visible light (*520nm*) portion of the spectrum, having a yellowish-green light (Figure 1). There is usually an overlap between the higher wavelength end of the excitation spectrum and the lower wavelength end of the emission spectrum. When electrons go from the excited state to the ground state, there is a loss of vibrational energy. As a result, the emission spectrum has an increased wavelength when compared to the excitation spectrum. This phenomenon is known as Stokes law or Stokes shift [30]. The greater the Stokes shift, the easier it is to separate the excitation light from the emission light. Since the excitation light must not disturb the measurement sensor (photomultiplier,

or PMT), the overlap between the excitation and emission wavelength is generally eliminated by an appropriate selection of optical filters.

In the present work, in order to achieve maximum intensity, the phosphorescent pigment particles was excited by the wavelength corresponding to the peak of the excitation curve, and the emission detection was selected at the peak wavelength of the emission curve. The selection of excitation and emission wavelengths was controlled by a UV lamp with a narrow wavelength range and an optical filter in the detection zone to eliminate the UV light that came from the lamp.

2.2. Experimental setup

2.2.1. Concentration measurement system

A "concentration measurement system" was developed to measure the tracer concentration in SiC/tracer mixtures. This system was composed of a vertical tube (PVC, ID=*38mm*, h=*300mm*) with two transparent sections for activation of the tracer particles and detection of the emission light. The lower section of the tube was equipped with a storage bin to collect the particles. This system was used under ambient temperature and in a darkroom. A schematic diagram of the setup is presented in Figure 2, where the feeding system, activation zone, vertical tube and detection zone are identified.

The activation zone:

In the activation zone, the sample goes through a funnel with an exit orifice of *1.5mm*, using a vibrating motor attached to the funnel to ensure a steady and low particle mass flow rate (≈ *6 g/min*). A *25W* UV-LED spot light source with an LED controller from Hamamatsu L11921-415, is directed right at the exit of the funnel. The emission spectrum of the UV light (*365 nm +/- 5nm*) fits around the maximum of the excitation spectrum of the tracer. It is very important that the light source chosen for the pigment excitation has sufficient power especially for very low pigment concentrations. A ventilator was used under the UV-LED light in order to prevent overheating of the lamp during the

experiment. The interior portion of the tube in the activation zone was covered by a reflective aluminum film in order to reflect the UV light toward the pigment particles and increase the activation efficiency of the system. As a consequence, all the particles had a proper excitation after leaving the activation zone.

The detection zone:

The detection zone is composed of four elements, a photomultiplier, a power supply system, an acquisition system and a UV filter. The photomultiplier (or PMT), Lynx Silicon Photomultiplier Module LynX-A-33-W50-T1-X, utilizes a *3×3mm*^{2} active area Silicon Photomultiplier (SiPM). The choice of this type of PMT is justified by its compatibility with the selected pigment because of its precision in the wavelength range from *350-950nm*, and peak of detection at *510nm.* The PMT was installed at the tube outlet at a distance of about *50mm* from the tube wall. This distance is close enough for detection of the pigment intensities and at the same time far enough from the wall such that it is not overwhelmed by the particles closest to the wall, therefore detecting all particles in the flow. The detection efficiency according to the wavelength, the emission spectrum of the UV light and the absorption and emission wavelength of Lumilux® Green SN-F50 WS are presented in Figure 1.
The UV filter, HOYA UV(0) L39, was placed between the PMT and the tube wall to reduce the signal of the UV LED detected by the PMT. This UV filter only eliminates the wavelength of the UV light so it increases the sensitivity of the detection system and allows low tracer concentrations to be measured, without being masked by the UV LED [1].

2.2.2. Calibration curve

The calibration of the “concentration measurement system” was carried out in order to provide the empirical relationship between the integral of the detected signal and the pigment concentration in the SiC/pigment mixture. To establish the calibration curve, SiC/pigment mixtures with different compositions (ranging from *0.25wt.%* to *6.25wt.%*) were prepared. The upper limit of the sample

concentration was set to *6.25wt.%* since it saturates the PMT maximum sensitivity. As a low consumption of tracer is desired, the measurements were carried out with the highest PMT sensitivity and very low pigment concentrations. For the calibration, *20 g* of the different samples (SiC/Pigment mixtures) with known compositions were injected into the concentration measurement system, through the funnel vibrating at a low mass flow rate (*≈6 g/min*). This low mass flow rate ensured that there was no particle superposition in front of the photomultiplier in the detection zone. After each measurement, the equipment was cleaned for *10* seconds with a vacuum cleaner.
It must be highlighted that this calibration curve focuses mainly on very low pigment concentrations, according to the objectives of this study: particles RTD measurement in solids unit operations with long residence time with minimum tracer consumption (minimal disturbance of the hydrodynamics of the studied system). Indeed, at higher pigment concentrations, the PMT sensor would reach saturation (maximum value). The PMT sensor could still be used for higher pigment concentrations but its sensitivity (which is adjustable) should be reduced to avoid saturation and a new calibration curve should be established under these conditions. However, for RTD measurements, low pigment concentrations are required in order to minimize the pigment consumption and to limit any disturbance of the hydrodynamics.
The measurements were repeated *5* times for each tracer concentration in order to estimate the repeatability and to ensure that there was no drifting of the concentration measurement system over time. The integral of the emitted light from each sample was related to the pigment concentration after eliminating the background noise from the raw signal (described in section 3.1)).
The operating parameters of the calibration procedure are reported in Table 3.

2.2.3. Methodology validation using RTD measurements in a bubbling fluidized bed

In order to validate the RTD measurement methodology, a bubbling fluidized bed was used to compare its experimental solids RTD with theoretical values. Figure 3 shows the schematic diagram of the experimental setup.

This fluidized bed consists of six main parts: fluidization column, air distributor, air flow controller, solids feeder, acquisition system and exit of the fluidized bed. The fluidization column is a Pyrex cylinder of *100mm* inner diameter and *480mm* height. The solids feed control system (feeding system), which consists of a funnel with a vibrating motor and a soft tube with a valve, allows us to have a controlled and stable solids flow rate. A solids exit channel with a *4mm* tube is located at the bottom of the fluidized bed at *30mm* above the air distributor. The air distributor is made of a perforated plate (*2mm* 176* holes, *7%* open area). The fluidization gas (air at ambient temperature; *23±2 °C* and the relative humidity of *7±1%*) is supplied from the compressor. Before entering into the fluidized bed, the compressed air passes through a filter, pressure regulator and a calibrated mass flow controller.

SiC particles were used as a bulk powder and phosphorescent tracer particles (Lumilux® Green SN-F50 WS) were used to determine the RTD of particles within the fluidized bed reactor. In order to measure the particles RTD in the fluidized bed, a given powder mass was initially introduced to the system such that the bed had a height to diameter ratio (H/D) between 1 and 2 (depending on the experiment), where *H* represents the height of the powder bed at fixed bed conditions (SiC and tracer particles) and *D* the diameter of the column. The tracer was premixed with the bulk powder (SiC) by fluidization during *5* minutes to ensure a homogenous mixture, with a total concentration of *6.25wt.%*.

A bubbling fluidized bed was used in this study since it is widely accepted that this type of fluidized beds is well described by the ideal CSTR model (continuous stirred tank reactor). Therefore, the RTD of a SiC/pigment mixture inside the fluidized bed column is expected to be similar to a CSTR model. It should also be mentioned that no slugging of the fluidized bed was observed, even for high H/D values, so that the fluidized bed could be assimilated to a CSTR. The initial concentration was selected to be as low as possible in order to have the lowest tracer consumption without loss of detection sensitivity. It should be noted that the low tracer concentration was necessary because high

concentrations would disturb the fluidization hydrodynamics and also, the tracer price could be an issue for the implementation of the technique in larger equipments.

In the present study, the pressure drop method was used to characterize the minimum fluidization velocity (U_{mf}) of the SiC powder. Figure 4 shows the pressure drop diagram at increasing and decreasing gas superficial velocities. The minimum fluidization velocity (U_{mf}) corresponds to the intersection between the upward sloping line (corresponding to a fixed bed) and the horizontal line (corresponding to a fluidized bed). When increasing the superficial velocity, it can be observed that the pressure rises slightly above the horizontal line corresponding to the fluidized state. This excess pressure is associated with the extra force required to overcome wall friction, interlocking of the particles or any "pre-compaction" of the powder (when filling the fluidization column). As a consequence, the minimum fluidization velocity (U_{mf}) was determined based on the pressure drop diagram at decreasing gas superficial velocities. Based on the experimental results, the minimum fluidization velocity (U_{mf}) of the SiC powder is approximately 6.3 mm/s (Figure 4).

Regarding the RTD characterization, three RTD curves were measured by varying the H/D ratio (1, 1.5 and 2, respectively) with the same fluidization velocity ($U/U_{mf} = 3$). These measurements were then used for the validation of the RTD measurement methodology. It should be noted that the samples were collected at the exit of the fluidized bed and then, the concentration measurement system was used in order to measure the concentration of the collected samples. As explained previously, the concentration measurement system was calibrated at a low mass flow rate (*6 g/min*) in order to obtain a low solid fraction in front of the detector (photomultiplier). Consequently, the concentration of the samples collected at the exit of the fluidized bed was measured in the exact same conditions. This procedure ensured that the same calibration curve could be used (because the solids fraction in front of the detector was the same for calibration and collected samples characterization).

Regarding the fluidization conditions ($U/U_{mf} = 3$), a range of $2 < U/U_{mf} < 5$ is typically used to obtain a smooth and regular bubbling fluidization behavior, with good mixing properties. Increasing the superficial gas velocity generally leads to better mixing properties, but also more elutriation (*i.e.*, entrainment of the particles). From a practical point of view, increasing the superficial gas velocity generally leads to better gas-solid heat and mass transfer characteristics, which can be relevant in many processes. In the present paper, it will be shown that at $U/U_{mf} = 3$, a RTD very close to the theoretical RTD of a perfectly mixed reactor (ideal CSTR model) is already obtained. Consequently, increasing the superficial velocity above $U/U_{mf} = 3$ would lead to very similar results (*i.e.*, similar RTD curves).

3. Results

3.1. Data post-treatment procedure

Figure 5 represents the measured raw signals of different SiC/pigment mixtures as a function of time. For each measurement, a data post-treatment procedure consisting of two main steps was applied:

- First, a 1st order Savitzky–Golay filter was applied to remove the noise from the measured signal. The smoothed signal was then used to calculate a baseline, from the instant when the PMT began detecting the emission of particles until no more emission was detected ;
- Secondly, the integral between the raw measured signal (without filtering) and the baseline was calculated. This integral is noted I and will be used to characterize the tracer concentration of different SiC/pigment mixtures.

3.2. Calibration curve

For the calibration curve (Figure 6), the measurements were repeated *5* times for each concentration, intercalating between the measurements of the RTD. This was done to ensure that there was no drifting in the measurements and that the calibration curve was reliable over time. The error bars

correspond to the 95% confidence intervals. A linear relation was obtained between the value of the integral of the PMT signal and the pigment concentration.

The linear fitting (passing through the origin) of the integral value with the tracer concentration in the mixture gives:

$$I = 38.62 \times C_{Pigment} \quad \text{Eq. (6)}$$

where I is the integral of the detected signal and $C_{Pigment}$ is the pigment concentration (wt.%) in the SiC/pigment mixture (using a constant sample mass of *20 g*).

It should be noted that the calculated value of the slope of the calibration curve (Eq. (6)) is valid under the conditions used in this work: minimum sensitivity of the PMT sensor, low and constant mass flow rate (same solids fraction in front of the detector), with a constant sample mass of 20 g (same signal length, as shown in Figure 5). Consequently, the concentrations of the samples collected at the exit of the fluidized bed (results presented in section 3.3) were measured in the exact same conditions to ensure that the same calibration curve could be used.

Generally speaking, the value of the slope could be affected by the mass flow rate, the sample mass and the sensitivity of the PMT sensor (which is adjustable). However, following the same procedure, a calibration curve corresponding to other conditions could easily be obtained.

3.3. RTD measurements

The present section describes and discusses the experimental results obtained from the fluidized bed RTD characterization. The RTD curves were determined experimentally by adding the tracer particles and measuring the variation in time of the pigment concentration at the exit. It should be recalled that the samples were collected at the output of the fluidized bed and then, the concentration measurement system was used in order to measure the concentration of the collected samples. These experimental RTD results were then compared to the theoretical ideal CSTR model (Eq. (4)) which is generally accepted as a valid description of the particles RTD in bubbling fluidized beds.

First, the repeatability of the RTD measurement technique developed in this work was evaluated by repeating the same RTD experiment for three times, with identical conditions: *1422 g* of SiC powder (which corresponds to a height to diameter ratio *H/D=1.5*), introduction of *95 g* of pigment, solid mass flow rate of 2.5 g/s. Figure 7 gives the F-curves (Eq. (2)) as a function of time for the three experiments. Vertical bars on the data points are the 95% confidence intervals for the cumulative distribution function (F-curves). These results show the good repeatability of the RTD characterization method proposed in this study.

Afterwards, the validity of this RTD measurement technique was evaluated by comparing the experimental results to the theoretical ideal CSTR model (Eq. (4)) for different *H/D* ratios of the fluidized bed. The operating conditions of these experiments are shown in Table 4. Figure 8 shows the experimental C-curves and F-curves as a function of time for the 3 values of the height to diameter ratio (*H/D*) of the fluidized bed. The theoretical curves corresponding to the ideal CSTR model (Eq. (4)) are also presented. The obtained data show a good agreement between the theoretical model and the experiments for all three H/D ratios. These results confirm that under the experimental conditions used in this study, the behavior of the experimental bubbling fluidized bed is very close to the theoretical ideal CSTR model (Eq. (4)), which is a commonly accepted result. Moreover, Table 5 presents a comparison of the experimental and theoretical mean residence times (t_m, Eq. (3)) and shows that the relative error is always lower than 6%. Consequently, these experiments confirm the validity of the RTD measurement technique developed in this work.

Finally, Table 6 reports the pigment mass balance, *i.e.*, a comparison between the masses of introduced pigment and “measured pigment” (*i.e.*, detected by the PMT), for the 3 values of the height to diameter ratio (*H/D*). The relative error is always close to 10% (maximum value = 12%) and it should be noted that the “measured pigment mass” is always lower than the introduced pigment mass. This could be explained by the elutriation (*i.e.*, entrainment) of the pigment particles and also

by their adhesion to the fluidized bed walls and concentration measurement system walls. Consequently, the main source of this relative error corresponds to inherent characteristics of the process (elutriation, attrition, adhesion, etc.) rather than the precision of the concentration measurement system.

Overall, the results presented in this section confirm the validity, repeatability and reliability of the developed methodology, which can be used for the characterization of particles RTD in solids unit operations, especially with long residence times.

4. Conclusions

A novel concentration measurement technique was developed in this study for measuring the particles RTD in solids unit operations. The procedure which was developed is well suited to solids unit operations with long residence times. Also, the presented technique eliminates the requirement of knowing the velocity and concentration profiles at the exit section of the system and is therefore more accurate than conventional methods. A bubbling fluidized bed was studied and the experimental RTD results were then compared to the theoretical ideal CSTR model in order to validate this RTD measurement method.

The following conclusions can be drawn based on the results obtained in this study:

- The tracer concentration measurement system has the ability to detect very low pigment concentrations (even lower than *0.5wt.%*). It is required to measure the RTD of solids unit operation with long residence times while maintaining a low consumption of tracer particles.
- The linear relationship between the integral of the PMT detected signal and pigment concentration was proven to be reliable.
- The experimental C-curves and F-curves of the fluidized bed reactor measured with the present RTD technique are in good agreement with the theoretical values (ideal CSTR model).

- The experimental values of the mean residence time were close to the theoretical mean residence time values, with small relative errors (less than 6%, as shown in Table 5).

Further investigation is required by integrating the tracer concentration measurement system at the exit of the fluidized bed reactor in order to perform continuous measurements. Also, the possibility of coating the bulk particles with a thin layer of phosphorescent material could be investigated, in order to avoid the difficulties of finding phosphorescent particles of the same physical properties as the bulk particles.

References

[1] A. T. Harris, J. Davidson, R. Thorpe, A novel method for measuring the residence time distribution in short time scale particulate systems, Chemical Engineering Journal, 89 (2002) 127-142.

[2] A. T. Harris, J. F. Davidson, R. B. Thorpe, Particle residence time distributions in circulating fluidised beds, Chemical Engineering Science, 58 (2003) 2181-2202.

[3] D. C. Guio-Perez, H. Hofbauer, T. Pröll, Effect of Ring-Type Internals on Solids Distribution in a Dual Circulating Fluidized Bed System — Cold Flow Model Study, American Institute of Chemical Engineering (AlChE Journal), 59 (2013) 3612-3623.

[4] P. Peltola, J. Ritvanen, T. Tynjälä, T. Pröll, T. Hyppänen, One-dimensional modelling of chemical looping combustion in dual fluidized bed reactor system, Int. J. Greenh. Gas Control, 16 (2013) 72-82.

[5] L. Wei, Y. Lu, J. Wei, Hydrogen production by supercritical water gasification of biomass: Particle and residence time distribution in fluidized bed reactor, Int. J. Hydrogen Energy, 38 (2013) 13117-13124.

[6] H. S. Fogler, Elements of Chemical Reaction Engineering, Prentice Hall PTR, 2006.

[7] R. D. Abellon, Z. I. Kolar, W. den Hollander, J. J. M. de Goeij, J. C. Schouten, C. M. van den Bleek, A single radiotracer particle method for the determination of solids circulation rate in interconnected fluidized beds, Powder Technology, 92 (1977) 53-60.

[8] P. A. Ambler, B. J. Milne, F. Berruti, D. S. Scott, Residence time distribution of solids in a circulating fluidized bed: Experimental and modelling studies, Chemical Engineering Science, 45 (1990) 2179-2186.

[9] S. Bhusarapu, M. Al-Dahhan, M. P. Dudukovic, Quantification of solids flow in a gas–solid riser:

single radioactive particle tracking, Chemical Engineering Science, 59 (2004) 5381-5386.

[10] W. Lin, C. E. Weinell, P. F. B. Hansen, K. Dam-Johansen, Hydrodynamics of a commercial scale CFB boiler-study with radioactive tracer particles, Chemical Engineering Science, 54 (1999) 5495-5506.

[11] S. Mahmoudi, J. Baeyens, J. Seville, The solids flow in the CFB-riser quantified by single radioactive particle tracking, Powder Technology, 211 (2011) 135-143.

[12] H. J. Pant, V. K. Sharma, S. Goswami, J. S. Samantray, I. N. Mohan, T. Naidu, Residence time distribution study in a pilot-scale gas–solid fluidized bed reactor using radiotracer technique, Journal of Radioanalytical and Nuclear Chemistry, 302 (2014) 1283-1288.

[13] C. W. Chan, J. P. K. Seville, D. J. Parker, J. Baeyens, Particle velocities and their residence time distribution in the riser of a CFB, Powder Technology, 203 (2010) 187-197.

[14] A. Avidan, J. Yerushalmi, Solids Mixing in an Expanded Top Fluid Bed, American Institute of Chemical Engineers (AlChE Journal), 31 (1985) 835-841.

[15] D. C. Guío-Pérez, T. Pröll, H. Hofbauer, Solids residence time distribution in the secondary reactor of a dual circulating fluidized bed system, Chemical Engineering Science, 104 (2013) 269-284.

[16] D. C. Guío-Pérez, T. Pröll, H. Hofbauer, Influence of ring-type internals on the solids residence time distribution in the fuel reactor of a dual circulating fluidized bed system for chemical looping combustion, Chemical Engineering Research and Design, 92 (2014) 1107-1118.

[17] P. Legile, Y. Gonthier, A.Bernis, G. Lacour, Détermination du temps de séjour des particules dans un lit fluidisé gaz-solide par tracage magnétique, Powder Technology, 66 (1991) 69-74.

[18] R. Andreux, G. Petit, M. Hemati, O. Simonin, Hydrodynamic and solid residence time distribution in a circulating fluidized bed: Experimental and 3D computational study, Chemical

Engineering and Processing: Process Intensification, 47 (2008) 463-473.

[19] H. P. Cui, M. Strabel, D. Rusnell, H. T. Bi, K. Mansaray, J. R. Grace, C. J. Lim, C. a. McKnight, D. Bulbuc, Gas and solids mixing in a dynamically scaled fluid coker stripper, Chemical Engineering Science, 61 (2006) 388-396.

[20] M. J. Rhodes, S. Zhou, T. Hirama, H. Cheng, Effects of Operating Conditions on Longitudinal Solids Mixing in a Circulating Fluidized Bed Riser, American Institute of Chemical Engineers (AlChE Journal), 37 (1991) 1450-1458.

[21] K. Smolders, J. Baeyens, Overall solids movement and solids residence time distribution in a CFB-riser, Chemical Engineering Science, 55 (2000) 4101-4116.

[22] B. Du, F. Wei, Lateral solids mixing behavior of different particles in a riser with FCC particles as fluidized material, Chemical Engineering and Processing: Process Intensification, 41 (2002) 329-335.

[23] A. T. Harris, R. B. Thorpe, J. F. Davidson, Stochastic modelling of the particle residence time distribution in circulating uidised bed risers, Chemical Engineering Science, 57 (2002) 4779-4796.

[24] A. T. Harris, J. F. Davidson, R. B. Thorpe, Influence of exit geometry in circulating fluidized-bed risers, American Institute of Chemical Engineering (AlChE Journal), 49 (2003) 52-64.

[25] A. Harris, J. F. Davidson, R. B. Thorpe, The influence of the riser exit on the particle residence time distribution in a circulating fluidised bed riser, Chemical Engineering Science, 58 (2003) 3669-3680.

[26] C. Huang, Z. Qian, M. Zhang, F. Wei, Solids mixing in a down-flow circulating fluidized bed of 0.418-m in diameter, Powder Technology, 161 (2006) 48-52.

[27] F. Wei, Z. Wang, Y. Jin, Z. Yu, W. Chen, Dispersion of lateral and axial solids in a cocurrent

downflow circulating fluidized bed, Powder Technology, 81 (1994) 25-30.

[28] C. Yan, Y. Fan, C. Lu, Y. Zhang, Y. Liu, R. Cao, J. Gao, C. Xu, Solids mixing in a fluidized bed riser, Powder Technology, 193 (2009) 110-119.

[29] T. Chen, W. I. Patterson, J. M. Dealy, On-line Measurement of Residence Time Distribution in a Twin-screw Extruder, International Polymer Processing, 10 (1995) 3-9.

[30] F. Yang, B. Henderson, K. P. O'donnell, The origin of the Stokes shift: The line shapes of quantum well exciton absorption and photoluminescence spectra, Physica B: Condensed Matter, 185 (1993) 362-365.

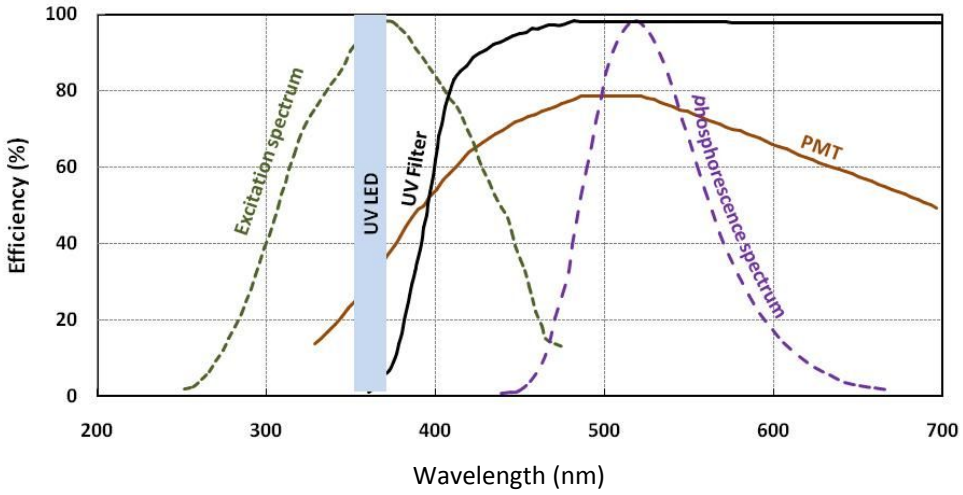

Figure 1: Lumilux® Green SN-F50 WS, PMT, UV filter and UV LED efficiency spectra (according to the pigment, PMT, UV filter and UV-LED characteristics indicated in the corresponding datasheets).

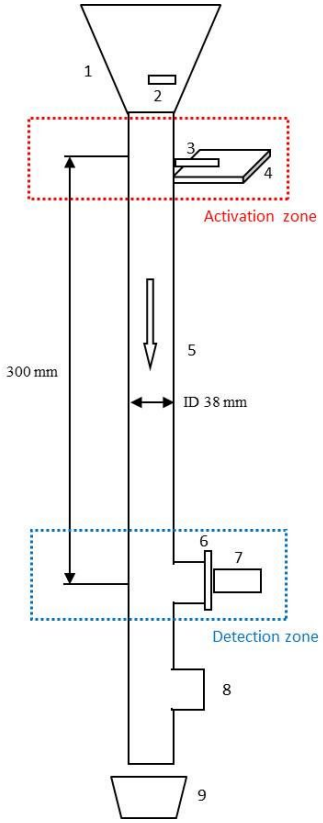

1. *Funnel*
2. *Vibrating motor*
3. *UV lamp*
4. *Ventilator*
5. *Vertical tube*
6. *UV filter*
7. *Photomultiplier*
8. *Vacuum cleaner connection*
9. *Storage bin*

Figure 2: Schematic diagram of the concentration measurement system.

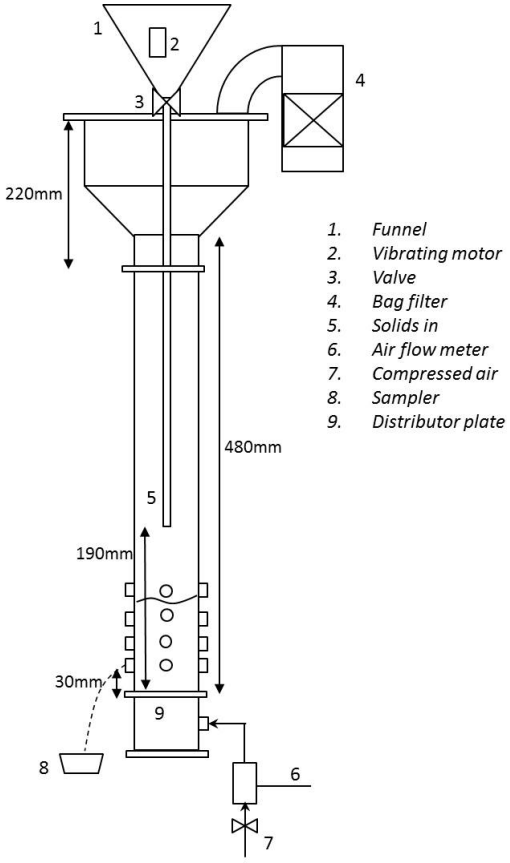

Figure 3: Schematic diagram of the experimental fluidized bed.

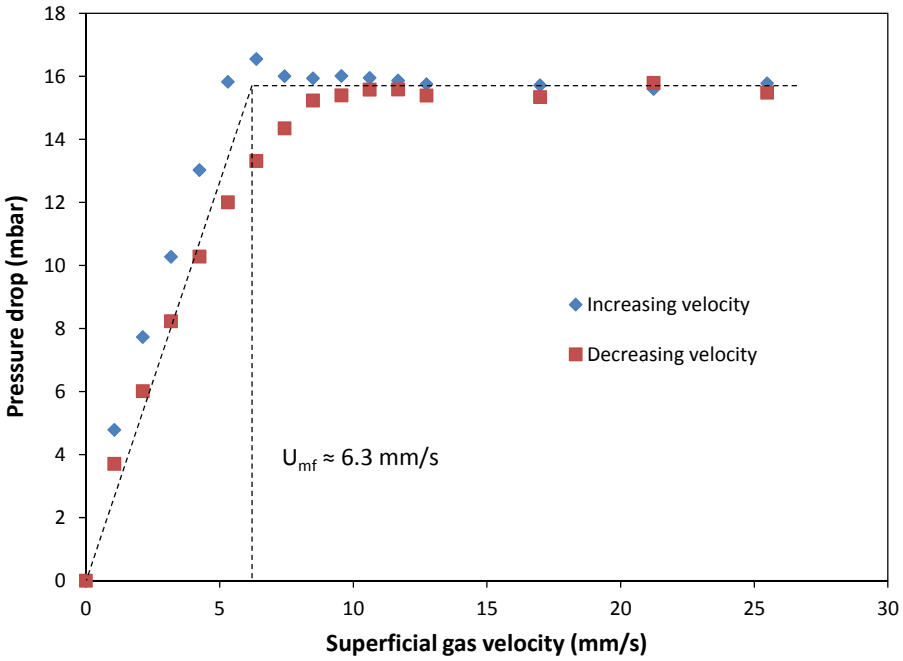

Figure 4: Pressure drop vs. superficial gas velocity (H/D=1.5; SiC mass=1422g).

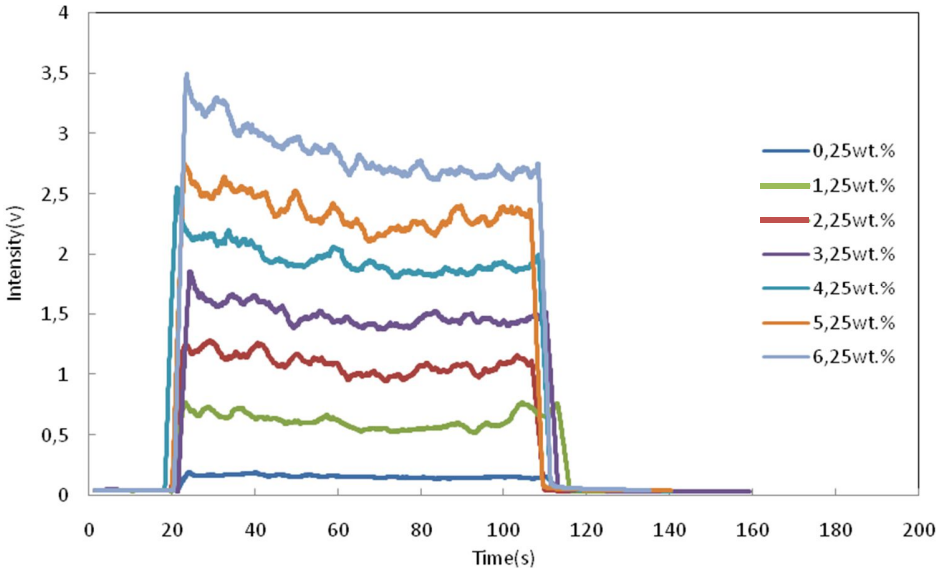

Figure 5: Measured raw signals for twenty grams of SiC/Pigment mixtures.

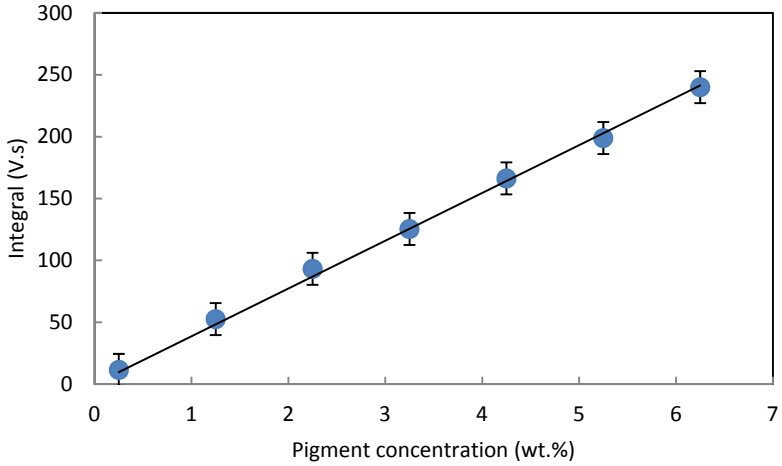

Figure 6: Calibration curve (Tracer concentration (wt.%) vs Integral of the PMT signal).

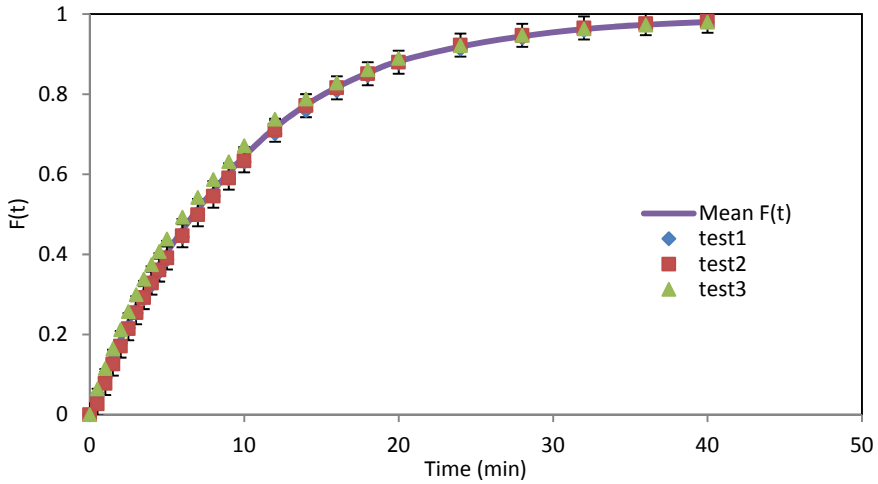

Figure 7: F(t) curves for identical conditions (H/D=1.5).

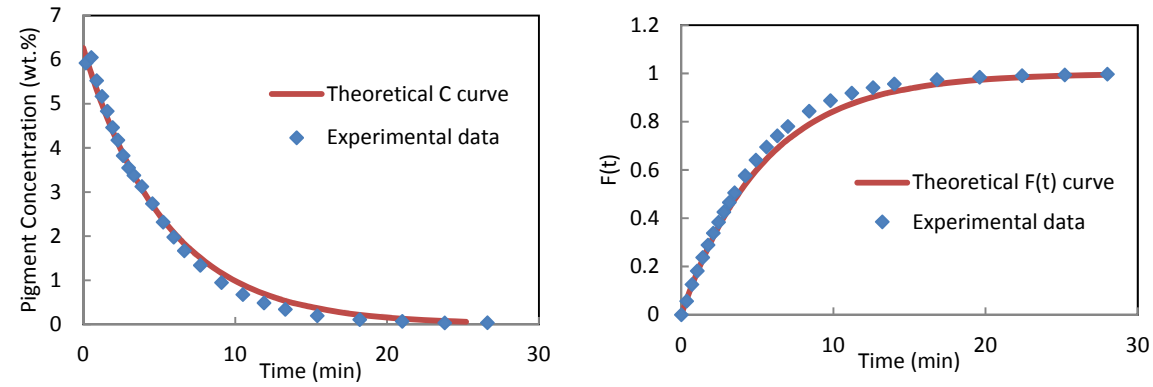

(a)

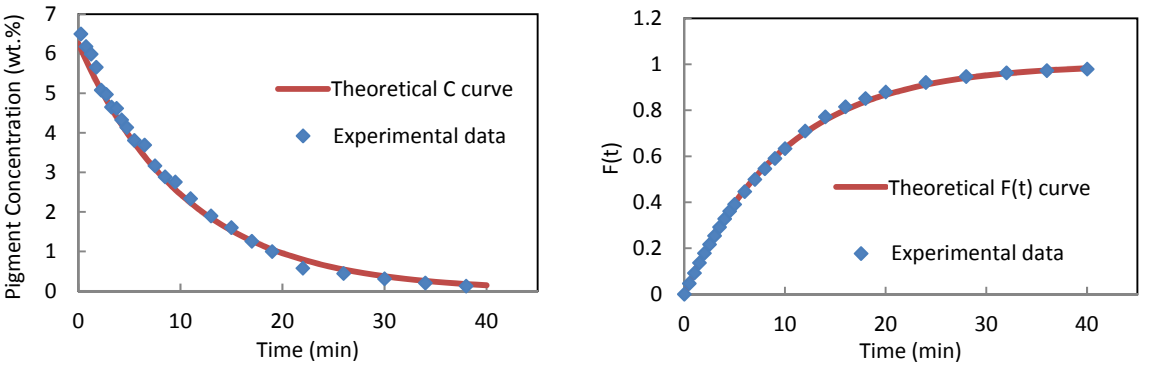

(b)

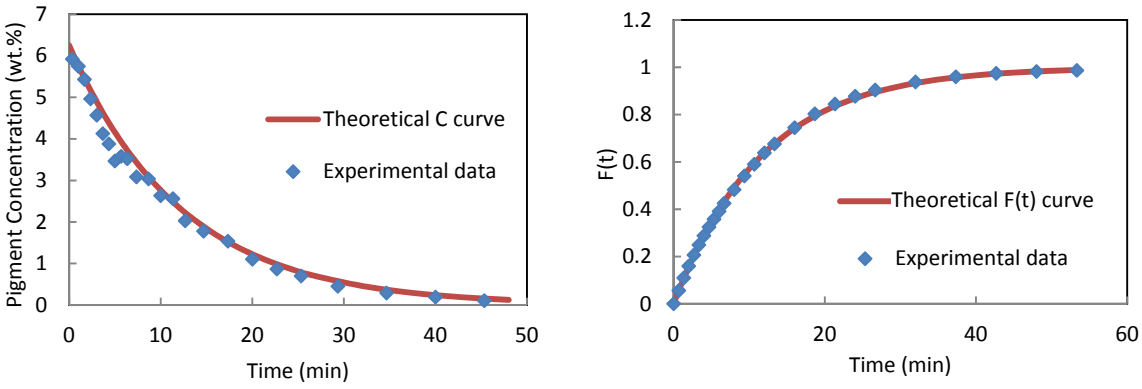

(c)

Figure 8: C (t) and F (t) of the fluidized bed as a function of time, compared to theoretical results for three different H/D values: (a) H/D = 1, (b) H/D = 1.5 and (c) H/D = 2.

Table 1: Summary of solids RTD methods.

Method	Authors	System	Details of the method
Radioactive tracer	Abellon et al. [7]	Four interconnected fluidized bed	Bed material: Glass beads Tracer: ^{24}Na and ^{192}Ir
	Ambler et al.[8]	CFB	Pulse tracer technique with Gallium-68 tracer
	Bhusarapu et al.[9]	Riser of CFB	Single radioactive particle (^{46}Sc)
	Lin et al. [10]	CFB boiler	^{56}Mn as tracer
	Mahmoudi et al.[11]	CFB riser	Positron emission particle tracking using ^{18}F as tracer
	Pant et al. [12]	Pilot scale fluidized bed reactor	Gold-198 as tracer
	Chan et al. [13]	Riser of fluidized bed	Positron emission particle tracking using^{18}F as tracer
Magnetic tracer	Avidan and Yerushalmi[14]	Expanded top fluidized bed	Ferromagnetic particle tracer
	Guío-Pérez et al. [15], [16]	Dual circulating fluidized bed	Steel particles as tracer
	Legile et al.[17]	Thin channel type gas-solid fluidized bed	Ferromagnetic particle tracer
Chemical particle tracer	Andreux et al. [18]	Riser of cold fluidized bed	NaClcrystals injected in the connecting point between L-valve and riser
	Cui et al. [19]	Stripper of fluidized bed	FCC particles were impregnated with a saturated solution of table salt and then dried to remove all moisture
	Rhodes et al. [20]	Riser of CFB	NaClas tracer; Tracer sampling was performed in three locations in the riser
	Smolders and Baeyens[21]	Riser of CFB	NaCl tracer
Phosphor particle tracer	Wei and Du [22]	Riser of CFB	The tracer particles are made by coating of fin phosphor particles on the surface of different property particles with nitryl-varnish as the bond.
	Harris et al. [1], [2], [23]–[25]	Riser of CFB	All particles have phosphorescent properties
	Huang et al.[26]	Down- flow CFB	A pneumatic injection phosphor tracer technique (PIPTT) was used to determine the axial and lateral solids dispersion by measuring the solids RTD at same axial but different lateral positions.
	Wei et al.[27]	CFB downer	A unique phosphor tracer technique measures the solids tracer concentration with time at different radial and axial positions within the co-current down flow circulating

			fluidized bed.
	Yan et al.[28]	Riser of CFB	The solids mixing in a riser with a height of 10 m and 0.186 m inner diameter was investigated by using the pneumatic phosphor tracer technique.
	Chen et al. [29]	Extruder	A He-Ne laser as a light source with carbon black as the tracer

Table 2: Physical properties of SiC and phosphorescent tracer powders.

Particle	D10	D50	D90	Sauter mean diameter D[3,2]	Density [g/cm^3]	Geldart Classification
Silicon Carbide (SiC)	41.4	72.7	122.2	58.3	3.22	A/B
Phosphorescent Tracer (Lumilux® Green SN-F50 WS)	40.9	70.4	120.3	64.5	3.63	A/B

Table 3: Operating conditions used for the calibration procedure.

Operating parameters	**Values**
Mass of the sample (g)	20
Pigment concentration (wt.%)	0 – 6.25
Mass flow rate (g/min)	6±1
Tube inner diameter (mm)	38
Tube length (mm)	300

Table 4: Experimental conditions used for particle RTD measurements in the fluidized bed.

Experiment Number	Height to diameter (H/D)	Solid mass flow rate (g/s)	SiC mass (g)	Initial pigment concentration (wt.%)
1	1	2.5±0.2	948	6.25
2	1.5	2.5±0.2	1422	6.25
3	2	2.5±0.2	1896	6.25

Table 5: Effect of the height to diameter ratio (H/D) on the mean residence time.

Height to diameter (H/D)	**Mean residence time (t_m) (min)**		
	Experimental	***Theoretical***	***Relative error (%)***
1	5.1 ± 0.4	5.40	5.6
1.5	10.1 ± 0.4	10.15	0.5
2	12.4 ± 0.4	12.26	1.1

Table 6: Pigment mass balance (comparison of the introduced and measured pigment masses).

Height to diameter (H/D)	**Pigment mass balance**		
	Introduced pigment (g)	***Measured pigment (g)***	***Relative error (%)***
1	63.3	56.5	10.7
1.5	95.0	83.6	12.0
2	126.4	112.1	11.3